Supporting Information

A Stepwise Targeting Curcumin Derivative, Ser@TPP@CUR, for Acute Kidney Injury

Xia Yan,[1,#] Xue-Ying Tan,[2,#] Yi-Xuan Li,[3] Hong-Bo Wang,[4] Jian-Bo Jin,[4] Ying-Rui Mao,[5] Jing-Bo Hu,*[,3] and Ling-Hui Wu*[,6]

[1] Li Dak Sum Yip Yio Chin Kenneth Li Marine Biopharmaceutical Research Center, Department of Marine Pharmacy, College of Food and Pharmaceutical Sciences, Ningbo University, Ningbo 315800, China.

[2] College of Pharmacy, Zhejiang Pharmaceutical College, Ningbo 315100, China.

[3] Faculty of Materials Science and Chemical Engineering, Ningbo University, Ningbo 315211, China.

[4] Department of pharmacy, Ningbo University affiliated Yangming Hospital, Yuyao 315400, China.

[5] Medical college, Ningbo University, Ningbo 315211, China.

[6] Department of Nephrology, The People's Hospital of Lishui, The Sixth Affiliated Hospital of Wenzhou Medical University, Lishui 323000, China.

[#] These authors contributed equally to this paper

[*] **Corresponding authors:**

Jingbo Hu, Faculty of Materials Science and Chemical Engineering, Ningbo University, Ningbo 315211, China. E-mail: hujiaabo@zju.edu.cn.

Ling-Hui Wu, Department of Nephrology, The People's Hospital of Lishui, The Sixth Affiliated Hospital of Wenzhou Medical University, Lishui 323000, China. E-mail: 18957091386@163.com.

Table of Contents

1. 1. Materials and methods....4
1.1. Materials....4
1.2. Synthesis and characterization of Ser@TPP@CUR....4
1.3. Synthesis of compound 1....4
1.4. Synthesis of compound 2....5
1.5. Synthesis of compound 3....5
1.6. Molecular docking....6
1.7. Cell culture....6
1.8. Immunofluorescence staining and Western blot of KIM-1 receptor....7
1.9. Uptake by LPS-stimulated HK-2 cells....7
1.10. Colocalization analysis on KIM-1 receptors....7
1.11. Co-localization analysis on mitochondria....7
1.12. Cell survival....8
1.13. Intracellular ROS detection....8
1.14. Bio-distribution....8
1.15. Establishment of AKI animal model....9
1.16. Assessment of renal function....9
1.17. Histological analysis....9
1.18. Preparation of mitochondria....9
1.19. ROS release measurements....10
1.20. Detection of inflammatory cytokines and oxidative stress....10
1.21. Statistical analysis....10
1.22. Copies of ^{1}H, ^{13}C, ^{31}P NMR and HRMS spectra....11
1.22.1 ^{1}H NMR spectrum of compound 1....11
1.22.2 ^{13}C NMR spectrum of compound 1....11
1.22.3 ^{31}P NMR spectrum of compound 1....12
1.22.4. ESI-HRMS of compound 1....12
1.22.5. ^{1}H NMR spectrum of compound 2....13
1.22.6. ^{13}C NMR spectrum of compound 2....13
1.22.7. ^{31}P NMR spectrum of compound 2....14

1.22.8. ESI-HRMS of compound 2 14
1.22.9. ^{1}H NMR spectrum of compound 3 15
1.22.10. ^{13}C NMR spectrum of compound 3 15
1.22.11. ^{31}P NMR spectrum of compound 3 16
1.22.12. ESI-HRMS of compound 3 16
1.22.13. The 2D binding mode of TIM1 and L-serine 17
1.22.14. The 2D binding mode of TIM1 and Ser@TPP@CUR 17
1.22.15. The expression of KIM-1 receptors on HK-2 cells 18
1.22.16. Co-localization analysis 18
1.22.17. Co-localization analysis 19
1.22.18. The semiquantitative fluorescence intensity 19
1.22.19. The semiquantitative fluorescence intensity 20

1. 1. Materials and methods

1.1. Materials

NMR spectra were recorded on a Bruker AV-600 spectrometer. High-resolution mass spectrometer (HRMS) were recorded on an Agilent 6230 TOF LC/MS system. Silica gel (300-400 mesh) for flash column chromatograph (FCC) and glass-backed thin-layer chromatography (TLC) plates were purchased from Sinopharm Chemical Reagent (Shanghai).

1.2. Synthesis and characterization of Ser@TPP@CUR

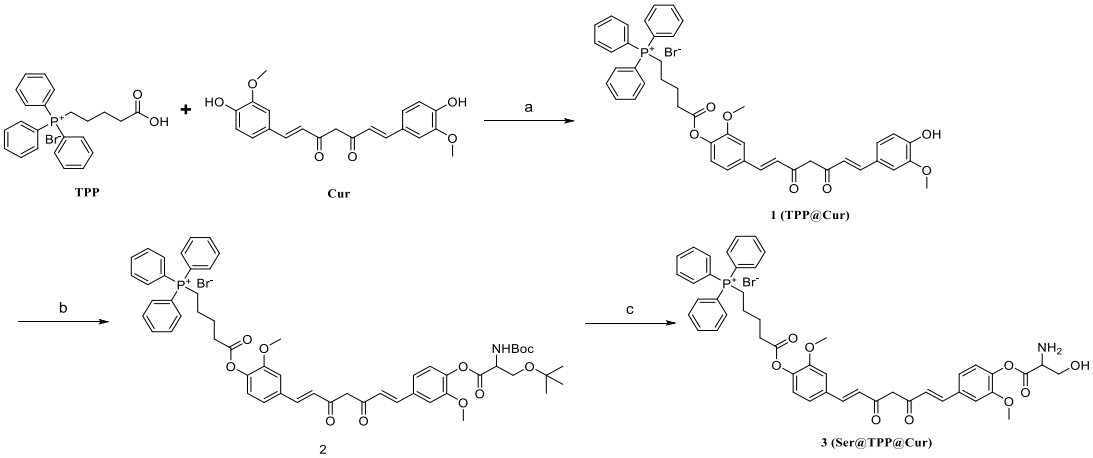

SScheme 1. The synthetic route of Ser@TPP@CUR.

1.3. Synthesis of compound 1

(5-(4-((1E,6E)-7-(4-hydroxy-3-methoxyphenyl)-3,5-dioxohepta-1,6-dien-1-yl)-2-methoxyphenoxy)-5-oxopentyl)triphenylphosphonium (1, TPP@CUR). To a round bottom flask was added Curcumin (1.00 g, 2.71 mmol), (4-Carboxybutyl)triphenyl phosphonium bromide (1.00 g, 2.26 mmol) and N,N'-dicyclohexylcarbodiimide (0.56 g, 2.71 mmol), 4-Dimethylaminopyridine (55 mg, 0.45 mmol). The flask was flushed with nitrogen, and then anhydrous DCM (15 mL) was added. The reaction was stirred for 12 h at room temperature. Then the mixture was filtered and concentrated, and purified by silica gel flash column chromatograph to afford compound 1 (TPP@CUR) 1.16 g in 65% yield as yellow solid (Figure S1, S2, S3 and S4). ^{1}H NMR (600 MHz, Chloroform-*d*) δ 8.33 (s, 1H), 7.78 (dd, *J* = 12.3, 7.4 Hz, 10H), 7.68 (dt, *J* = 10.0, 4.9 Hz, 7H), 7.57 (t, *J* = 17.0 Hz, 2H), 7.07 (dd, *J* = 17.8, 7.9 Hz, 4H), 6.94 (d, *J* = 8.0 Hz, 2H), 6.53 (dd, *J* = 39.3, 15.7 Hz, 2H), 3.93 (s, 3H), 3.75 (s, 2H), 3.72 (s, 3H), 2.69 (t, *J* = 6.9 Hz, 2H), 2.10 (t, *J* = 7.4 Hz, 2H), 1.84 (q, *J* = 8.0 Hz, 2H). ^{13}C NMR (151 MHz, Chloroform-*d*) δ 184.64, 181.78, 171.03, 163.06,

151.27, 148.22, 146.97, 141.26, 141.06, 139.24, 135.20, 135.18, 134.12, 133.68, 133.61, 130.62, 130.54, 127.47, 124.40, 123.20, 121.71, 121.07, 118.41, 117.83, 114.98, 111.42, 109.74, 101.68, 56.04, 55.98, 32.95, 25.54, 25.42, 22.75, 22.42, 21.78, 21.75.^{31}P NMR (243 MHz, Chloroform-*d*) δ 24.10. ESI-HRMS: calcd.for $C_{44}H_{42}O_7P$ $[M-Br]^+$: 713.2663, found: 713.2669.

1.4. Synthesis of compound 2

(5-(4-((1E,6E)-7-(4-((N-(tert-butoxycarbonyl)-O-(tert-butyl)seryl)oxy)-3-methoxyphenyl)-3,5-dioxohepta-1,6-dien-1-yl)-2-methoxyphenoxy)-5-oxopentyl)triphenylphosphonium (2). To a round bottom flask was added 1 (TPP@CUR, 1.00 g, 1.26 mmol), EDCI (0.25g, 1.32 mmol), HOBT(0.18 g, 1.32 mmol), DIEA (0.17 g, 1.32 mmol) and N-(tert-butoxycarbonyl)-O-(tert-butyl)serine (0.59 g，1.32 mmol）in CH_2Cl_2 (10 mL). The mixture was stirred for 12 h at room temperature. The reaction mixture was quenched with 0.1 M HCl, extracted with CH_2Cl_2 (3 x 30 mL), dried over Na_2SO_4, concentrated and purified by silica gel flash column chromatograph to afford compound 2 235 mg in 18% yield as yellow solid (Figure S5, S6, S7 and S8). ^{1}H NMR (600 MHz, Chloroform-d) δ 8.32 (s, 1H), 7.81 – 7.78 (m, 10H), 7.70 (d, J = 8.2 Hz, 7H), 7.61 (dd, J = 15.8, 9.5 Hz, 2H), 7.16 – 7.07 (m, 4H), 6.97 (d, J = 8.1 Hz, 2H), 6.59 (d, J = 15.8 Hz, 2H), 5.48 (d, J = 9.0 Hz, 1H), 4.69 (d, J = 9.2 Hz, 1H), 4.03 – 3.98 (m, 1H), 3.87 (s, 3H), 3.78 (d, J = 8.1 Hz, 2H), 3.74 (s, 3H), 2.71 (t, J = 7.1 Hz, 2H), 2.11 (q, J = 7.5 Hz, 2H), 1.85 (t, J = 8.0 Hz, 2H), 1.47 (d, J = 7.6 Hz, 9H), 1.22 (t, J = 4.3 Hz, 9H). ^{13}C NMR (151 MHz, Chloroform-d) 183.29, 183.23, 173.23, 171.13, 169.27, 163.15, 155.75, 151.56, 151.41, 141.34, 141.31, 140.12, 139.98, 135.28, 135.26, 134.12, 134.10, 133.79, 133.77, 133.73, 133.71, 130.74, 130.71, 130.65, 130.62, 124.48, 124.42, 123.42, 123.35, 121.29, 121.19, 118.54, 117.97, 111.75, 111.56, 102.04, 80.15, 73.62, 62.19, 60.53, 56.09, 56.04, 54.46, 33.34, 33.05, 28.45, 27.50, 25.62, 25.51, 22.83, 22.81, 22.51, 22.49, 21.88, 21.85, 14.30. ^{31}P NMR (243 MHz, Chloroform-d) δ 24.12. ESI-HRMS: calcd.for $C_{56}H_{63}NO_{11}P$ $[M-Br]^+$: 956.4133, found: 956.4175.

1.5. Synthesis of compound 3

(5-(2-methoxy-4-((1E,6E)-7-(3-methoxy-4-(seryloxy)phenyl)-3,5-dioxohepta-1,6-dien-1-yl)phenoxy)-5-oxopentyl)triphenylphosphonium (3, TPP@Cur@Ser). TFA (2 mL) was added dropwise with stired to a solution of compound 2 (216 mg, 0.2 mmol) in dichloromethane (2 mL) at ice bath. The reaction mixture was stirred for 8 h at room temperature. The mixture was

concentrated, then recrystallized in dichloromethane/ diethyl ether to afford the pure products compound 3(Ser@TPP@CUR) 190 mg in 95% yield as yellow solid (Figure S9, S10, S11 and S12). ^{1}H NMR (600 MHz, DMSO-d6) δ 8.82 – 8.44 (m, 2H), 7.91 (t, J = 7.5 Hz, 3H), 7.85 – 7.71 (m, 14H), 7.66 (dd, J = 15.9, 6.1 Hz, 1H), 7.58 (s, 1H), 7.50 (s, 1H), 7.36 (dd, J = 36.2, 8.2 Hz, 2H), 7.23 (d, J = 8.2 Hz, 1H), 7.13 – 6.92 (m, 3H), 5.85 (s, 1H), 4.50 (d, J = 4.2 Hz, 1H), 4.04 (s, 1H), 3.95 (d, J = 11.2 Hz, 1H), 3.85 (d, J = 14.4 Hz, 3H), 3.74 (s, 2H), 3.66 (dt, J = 14.9, 7.5 Hz, 3H), 2.68 (d, J = 7.4 Hz, 2H), 1.90 – 1.81 (m, 2H), 1.68 (q, J = 8.0 Hz, 2H). ^{13}C NMR (151 MHz, DMSO-d6) δ 183.46, 183.03, 170.70, 166.60, 158.09, 157.88, 151.16, 150.92, 140.88, 139.97, 139.61, 135.00, 134.49, 133.76, 133.66, 133.59, 130.37, 130.29, 125.10, 124.69, 123.27, 123.09, 121.53, 121.46, 118.82, 118.37, 118.25, 116.37, 112.47, 112.15, 101.86, 59.66, 56.19, 56.00, 54.34, 48.64, 32.25, 25.35, 25.23, 21.10, 21.08, 20.16, 19.82.^{31}P NMR (243 MHz, DMSO-d6) δ 23.86. ESI-HRMS: calcd.for $C_{47}H_{47}NO_9P$ $[M-Br]^+$: 800.2983, found: 800.3008

1.6. Molecular docking

Docking studies were carried out using Autodock Vina program[1]. Docking was performed to obtain a population of possible conformations and orientations for the ligand at the binding site. The protein was converted to PDBQT file that contains a protein structure with hydrogens in all polar residues. All bonds of ligands were set as rotatable. All calculations for protein-fixed ligand-flexible docking were done using the Lamarckian Genetic algorithm (LGA) method. The hot residues reported in literature [2](Arg106, Trp112, Phe113, Asn114, Asp115, Lys117) were defined as the binding site of KIM-1. AutoDock Vina Extended automatically calculates the grid maps and clusters the results in a way transparent to the user. The best conformation was chosen with the lowest binding energy, after the docking search completed. The interactions complex protein-ligand conformations, including hydrogen bonds and the bond lengths were analyzed using PyMol.

1.7. Cell culture

HK-2 cells were purchased from the American Type Culture Collection (ATCC, Manassas, VA, USA) and cultured. Briefly, cells were passaged every 3–4 days in 100-mm dishes using Dulbecco's modified Eagle's medium-F12 supplemented with 10% fetal bovine serum, 100 U/mL penicillin, and 100 mg/mL streptomycin. These cells were incubated in a humidified atmosphere of 5% CO_2, 95% air at 37 ℃ for 24 h.

1.8. Immunofluorescence staining and Western blot of KIM-1 receptor

The expression of KIM-1 receptors during AKI was evaluated from the cellular level. HK-2 cells were inoculated into a 12-well plate at a density of 5×10^4 cells per well, and after the cells were adherent to the wall, 15 μg/mL LPS was added and co-incubated for 12 h. The expression of KIM-1 receptors on the cell surface of HK-2 cells after LPS-induced inflammation was examined, HK-2 cells without LPS pretreatment as control. The expression of KIM-1 receptors were examined by western blot.

1.9. Uptake by LPS-stimulated HK-2 cells

HK-2 cells were used as model cells to investigate the internalized behavior of Ser@TPP@CUR. They were inoculated into a 12-well plate at a density of 5×10^4 cells per well and incubated for 24 h. Cells were pretreated with 15 μg/mL LPS for 12 h and then incubated with Ser@TPP@CUR (CUR, 3 μg/mL) for 2 h and 6 h, CUR, Ser@CUR, TPP@CUR as control. After that the cells were fixed with methanol at -20°C, and then sealed and observed by an inversed fluorescent microscope (Axio Observer 5, Zeiss, Germany).

1.10. Colocalization analysis on KIM-1 receptors

HK-2 cells with LPS-induced inflammation were used to examine whether the entry of Ser@TPP@CUR into cells is mediated by the KIM-1 receptor. HK-2 cells were incubated into a 12-well plate at a density of 5×10^4 cells per well and incubated for 24 h. After pretreatment with 15 μg/mL LPS for 6 h, a culture medium containing free CUR and Ser@TPP@CUR (CUR, 3 μg/mL) was adopted for incubation for another 2 h. Cells were fixed with methanol at -20°C, the KIM-1 receptor was labeled by immunofluorescent staining and observed under an inversed fluorescent microscope, and a co-localization analysis was conducted by Image J.

1.11. Co-localization analysis on mitochondria

Fluorescence imaging was employed to examine whether Ser@TPP@CUR has mitochondrial targeting property. HK-2 cells were inoculated into a 12-well plate at a density of 5×10^4 cells per well and incubated for 24 h. After pretreatment with 15 μg/mL LPS for 12 h, a culture medium containing free CUR and Ser@TPP@CUR (CUR, 3 μg/mL) was adopted for incubation for another 6 h. Then Mito-Tracker-Red-CMXRos-kit was adopted for fluorescence labeling of mitochondria

of HK-2 cells. Cells were fixed with methanol at - 20 ◦C, then sealed and observed under an inversed fluorescent microscope, and a co-localization analysis was conducted by Image J.

1.12. Cell survival

To investigate whether Ser@TPP@Cur treatment protects HK-2 cells from endotoxin damage, a CCK-8 assay was used to assess cell survival. HK-2 cells were inoculated in a 96-well plate at a density of 5×10^3 cells per well and incubated for 24 h. DMEM/F12 serum-free medium containing 15 μg/mL LPS was adopted and Ser@TPP@CUR (CUR, 3 μg/mL) was added for incubation for a total of 24 h, CUR, Ser@CUR, TPP@CUR as control. After that, 15 μL MTT solution (5.0 mg/mL) was added to each well and incubated further for 4 h at 37°C. The media were removed and 200 μL DMSO was added to dissolve MTT formazan. After shaken for 20 min, the absorbance of formazan at 570 nm was measured with a microplate reader (Thermo FC), and viability was expressed as the percentage of the control.

1.13. Intracellular ROS detection

Intracellular ROS production in HK-2 cells was detected to assess whether Ser@TPP@Cur could effectively reduce the ROS level in inflammatory HK-2 cells. HK-2 cells were inoculated in a 12-well plate at a density of 5×10^4 cells per well and incubated for 24h. After pretreatment with 15 μg/mL LPS for 24h, a culture medium containing free CUR, TPP@Cur, Ser@Cur or Ser@TPP@Cur (CUR, 3 μg/mL) was adopted for incubation for another 2 h. Intracellular ROS production was measured using CellROX™ Deep Red Reagent (Invitrogen, USA) according to the manufacturer's instructions. Cells were fixed with methanol at -20°C, then sealed and observed under an inversed fluorescent microscope, and semi-quantitative analysis was conducted by Image J software.

1.14. Bio-distribution

Fluorescence imaging technology was used to investigate the bio-distribution of Ser@TPP@Cur, AKI mice as model animals. Since the compound Ser@TPP@CUR was readily decomposed to curcumin under strong acidic conditions, Ser@TPP@Cur (CUR, 4 mg/kg) was injected intravenously and the mice were executed at different time points after administration. Tissue samples including heart, liver, spleen, lung, and kidney were collected, and the distribution of CUR in each tissues was observed using the IVIS Lumia III In-Vivo imaging

system (PerkinElmer, USA). Then, the organ tissues were fixed in 4.5% formalin for freeze sectioning, and the distribution fluorescence of the drug in the tissues was observed under an inversed fluorescent microscope (Axio Observer 5, Zeiss, Germany).

1.15. Establishment of AKI animal model

All animal experiments were conducted in accordance with the ARRIVE Guideline and the guidelines of the US National Institutes of Health for the care and use of laboratory animals, and all animal experiments were approved by the Animal Ethics Committee of Ningbo University. In this study, Balb/c male mice were used as model animals for AKI induction via intraperitoneal injection of 10 mg/kg LPS.

The mice were randomly divided into five groups and i.v. administrated with corresponding drugs: (1) Control (n=6); (2) AKI (n=6); (3) AKI + CUR (n=6); (4) AKI + TPP@CUR (n=6); (5) AKI + Ser@CUR (n=6); (6) AKI + Ser@TPP@CUR (n=6). After 12 h administration, the mice were sacrificed and the blood samples and kidney tissues were harvested for the following measurements.

1.16. Assessment of renal function

The renal function of AKI mice was evaluated by detecting serum creatinine (Scr) and blood urea nitrogen (BUN) levels. Scr and BUN in serum samples of the laboratory mice were measured using an automated biochemical analyzer (Roche Diagnostics, Germany).

1.17. Histological analysis

The kidney tissue samples of the mice were fixed in 4% formalin solution for 24 h before embedded by paraffin and sectioned. Tissue sections were dewaxed and hydrated sequentially and stained with hematoxylin and eosin (H&E), and the histopathological changes in the kidneys were observed by an optical microscope (Primostar 3, Zeiss, Germany).

1.18. Preparation of mitochondria

Mitochondrial fractions were isolated from kidneys using mitochondria isolation kits according to the manufacturer’s instructions (Invitrogen, USA). Briefly, 200 mg kidney tissue was homogenized in 5 mL extraction buffer (10 mM HEPES, pH 7.5, containing 200 mM mannitol, 70 mM sucrose and 1 mM EGTA) with a homogenizer powered by an overhead electric motor at 200 g, and the pestle was moved up and down 5–10 times to ensure the total homogenization. The

homogenate was centrifuged at 800 g for 10 min to precipitate the nuclear fraction. The supernatant was then centrifuged at 7000 g for 10 min to yield the mitochondrial fraction. The mitochondrial pellet was suspended in 0.5 mL storage buffer (10 mM HEPES, pH 7.4, containing 250 mM sucrose, 1 mM ATP, 0.08 mM ADP, 5 mM sodium succinate, 2 mM K_2HPO_4 and 1 mM dithiothreitol). For assays, protein concentration was adjusted to 1.5~2.0 mg/mL. All procedures were carried out at 0~2°C.

1.19. ROS release measurements

ROS production in isolated mitochondria was measured using the Amplex Red Hydrogen Peroxide/Peroxidase Assay Kit (Invitrogen, USA) according to the manufacturer's instructions. Mitochondrial suspensions were incubated in the presence of 50 μM Amplex Red and 0.1 U/mL horseradish peroxidase, and fluorescence was monitored over time using a temperature-controlled (37°C) spectrofluorometer (Hitachi, Japan) operating at excitation and emission wavelengths of 544 and 590 nm, respectively, with gentle continuous stirring.

1.20. Detection of inflammatory cytokines and oxidative stress

The anti-inflammatory effects of Ser@TPP@Cur in AKI mice were evaluated by measuring TNF-α and IL-6 levels according to the manufacturer's instructions (Boster Co., Ltd., China).

The changes of superoxide dismutase (SOD), glutathione (GSH) and malondialdehyde (MDA) in renal tissues of AKI mice were measured by commercial kits (Nanjing jiancheng Bioengineering Institute, China)

1.21. Statistical analysis

All data are expressed as the mean ± SD. Statistical significance between two groups was assessed using Student's t-tests. $p < 0.05$ was considered significant.

1.22. Copies of ^{1}H, ^{13}C, ^{31}P NMR and HRMS spectra

1.22.1 ^{1}H NMR spectrum of compound 1

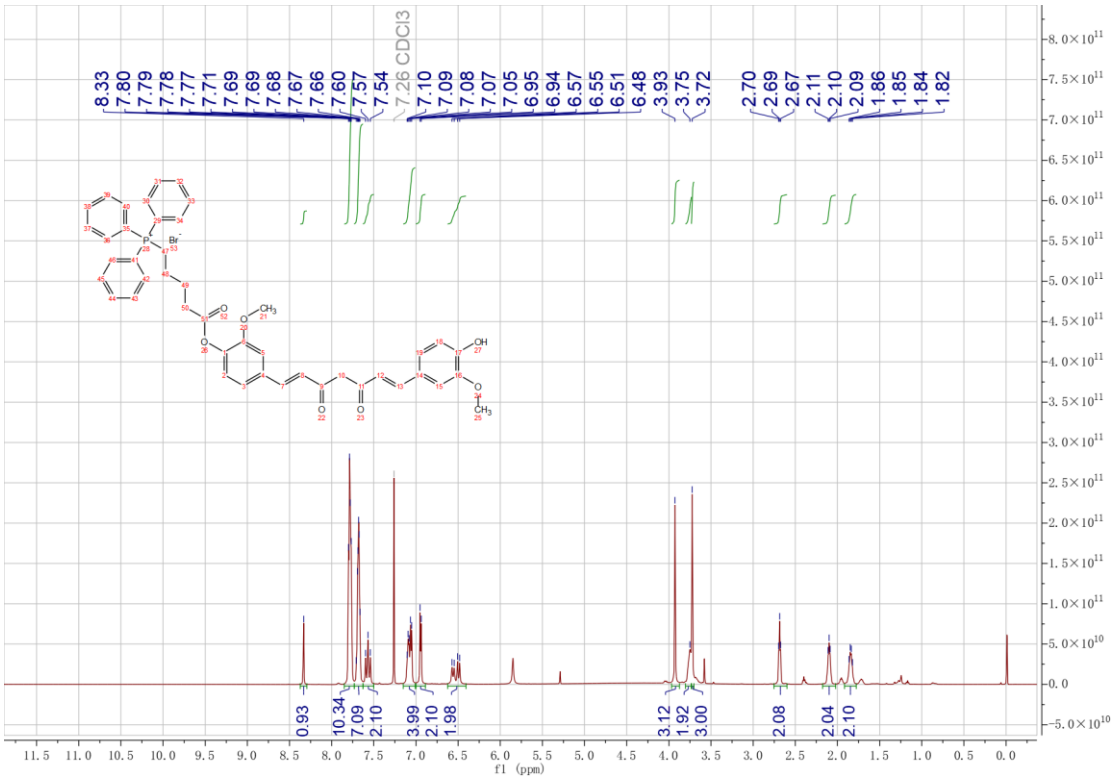

Fig. S1 ^{1}H NMR spectrum of compound 1 in $CDCl_3$.

1.22.2 ^{13}C NMR spectrum of compound 1

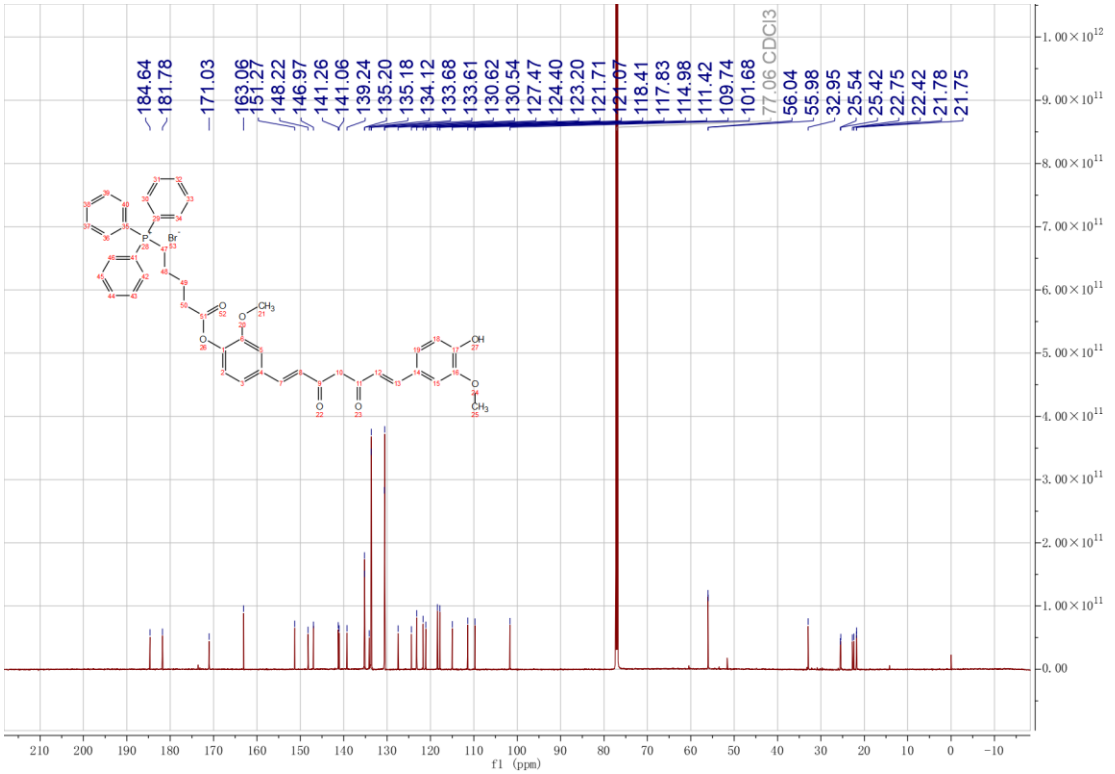

Fig. S2 ^{13}C NMR spectrum of compound 1 in $CDCl_3$.

1.22.3 ^{31}P NMR spectrum of compound 1

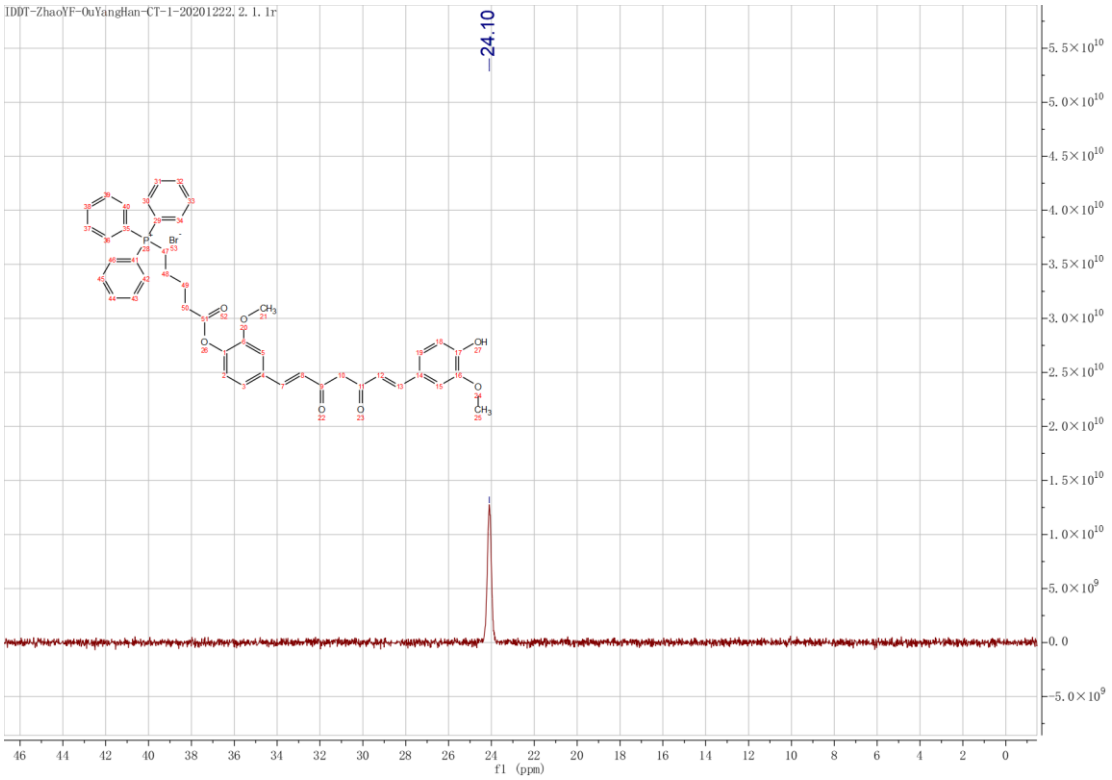

Fig. S3 ^{31}P NMR spectrum of compound 1 in $CDCl_3$.

1.22.4. ESI-HRMS of compound 1

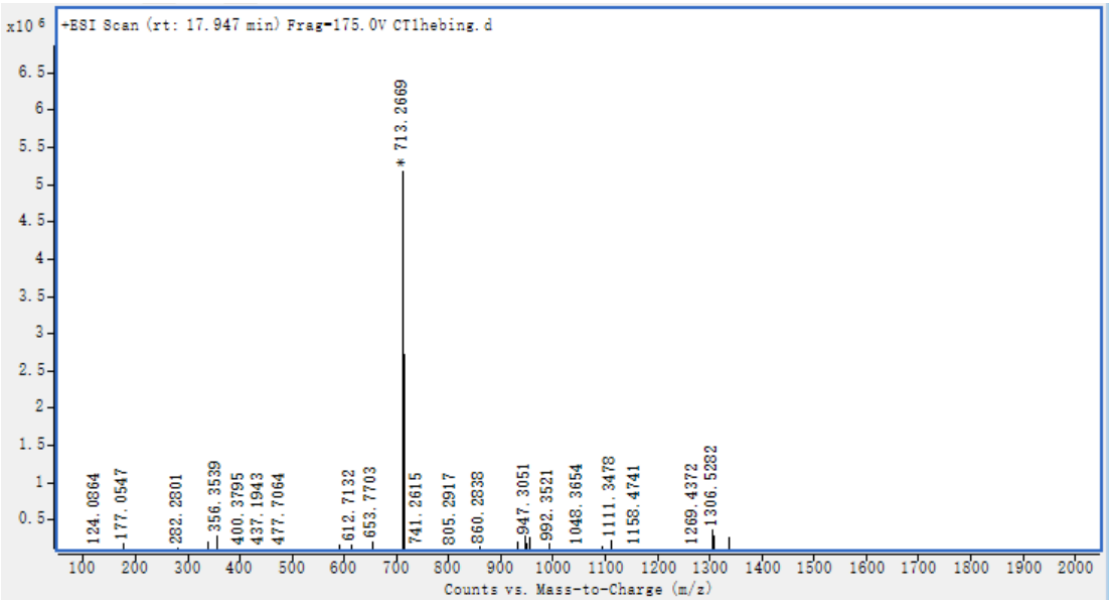

Fig. S4 ESI-HRMS of compound 1.

1.22.5. ^{1}H NMR spectrum of compound 2

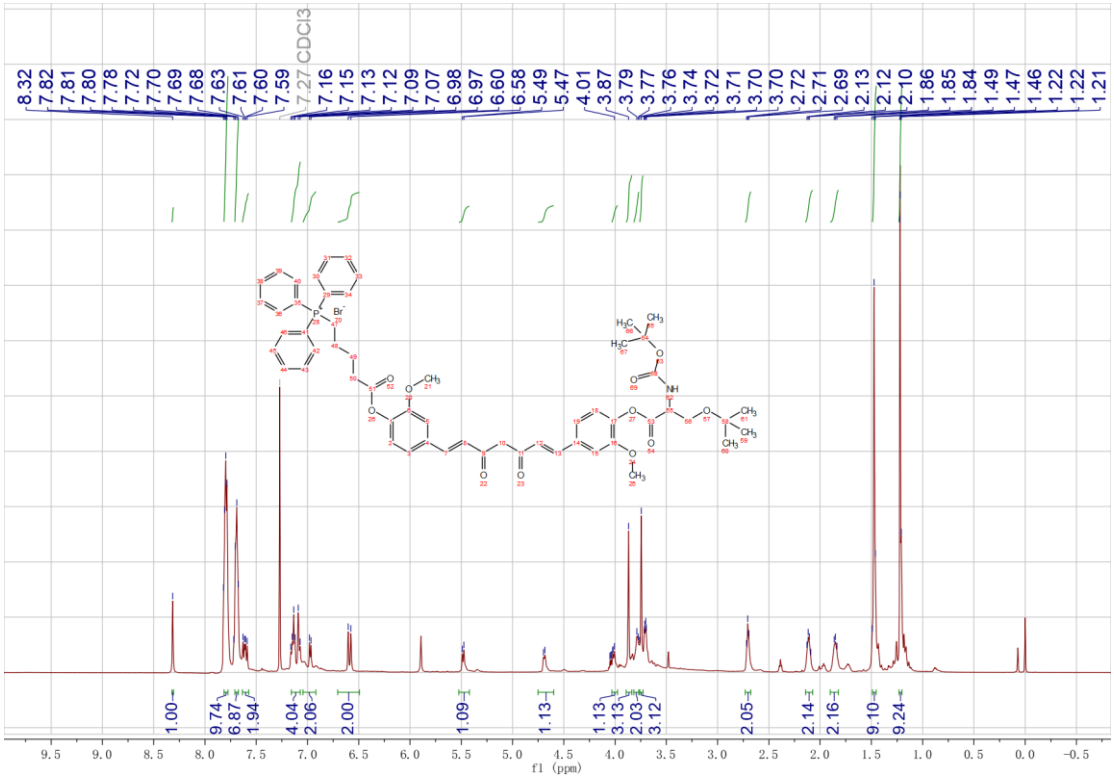

Fig. S5 ^{1}H NMR spectrum of compound 2 in $CDCl_3$.

1.22.6. ^{13}C NMR spectrum of compound 2

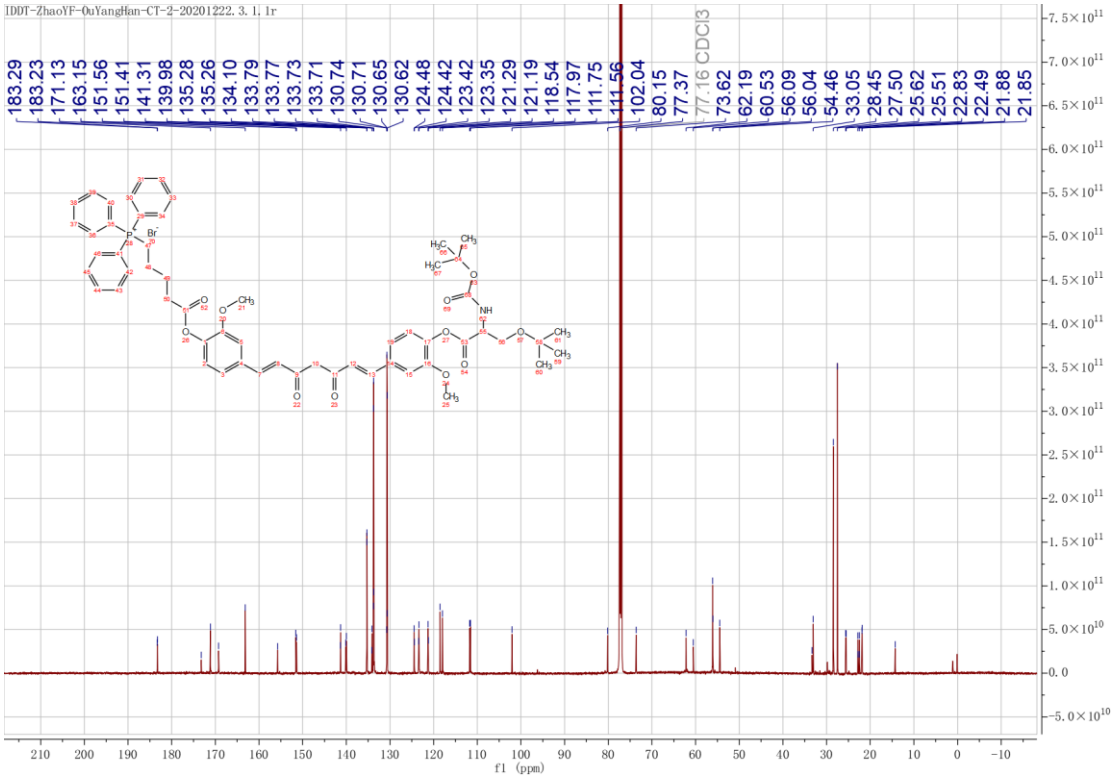

Fig. S6 ^{13}C NMR spectrum of compound 2 in $CDCl_3$.

1.22.7. ^{31}P NMR spectrum of compound 2

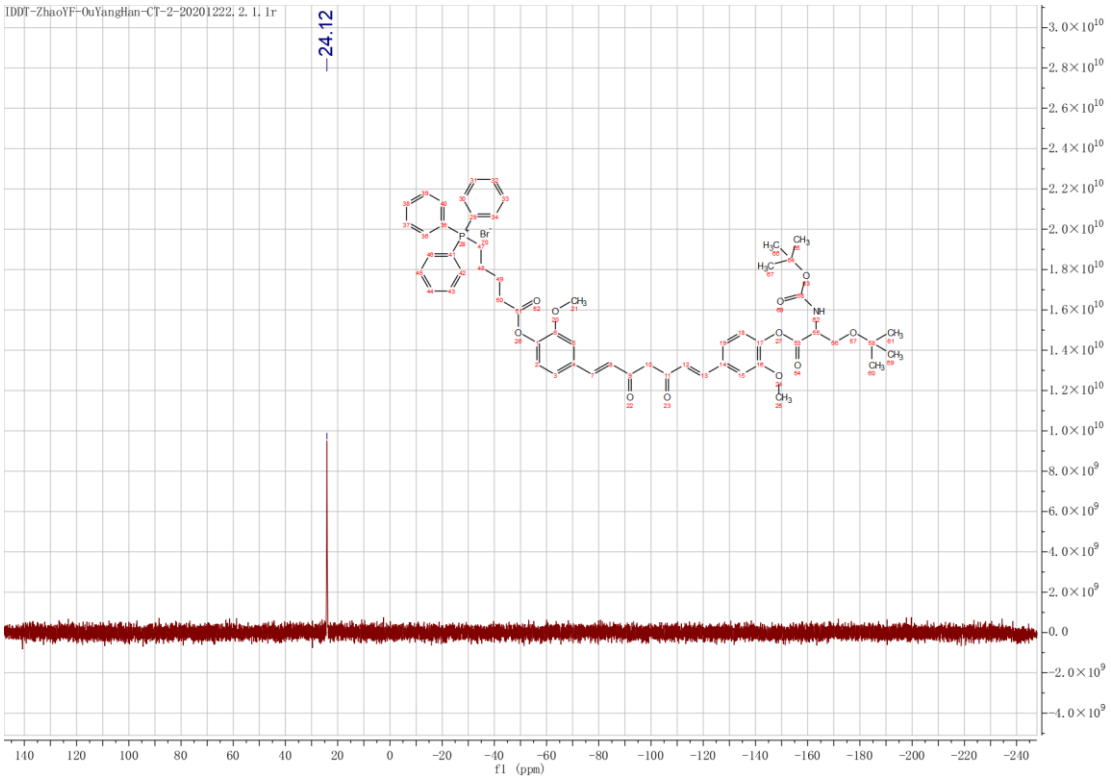

Fig. S7 ^{31}P NMR spectrum of compound 2 in $CDCl_3$.

1.22.8. ESI-HRMS of compound 2

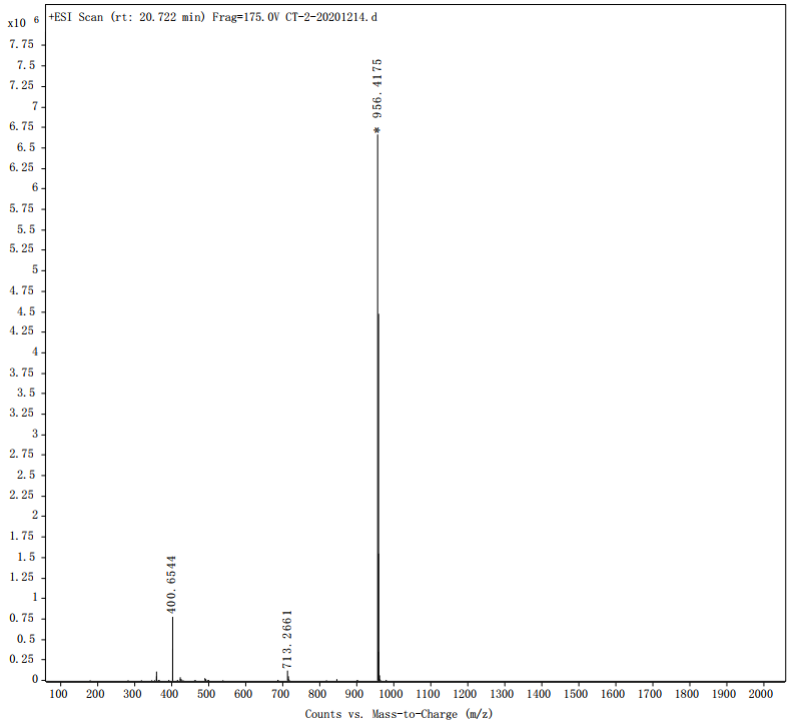

Fig. S8 ESI-HRMS of compound 2.

1.22.9. ^{1}H NMR spectrum of compound 3

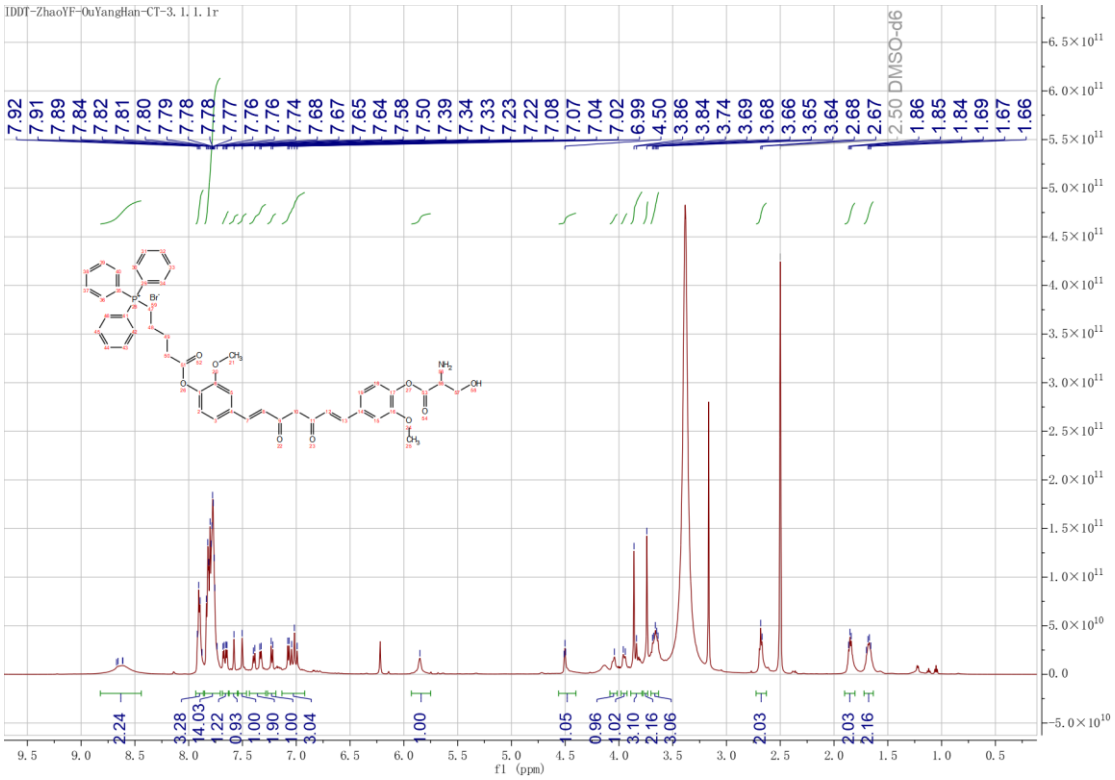

Fig. S9 ^{1}H NMR spectrum of compound 3 in $(CD_3)_2SO$.

1.22.10. ^{13}C NMR spectrum of compound 3

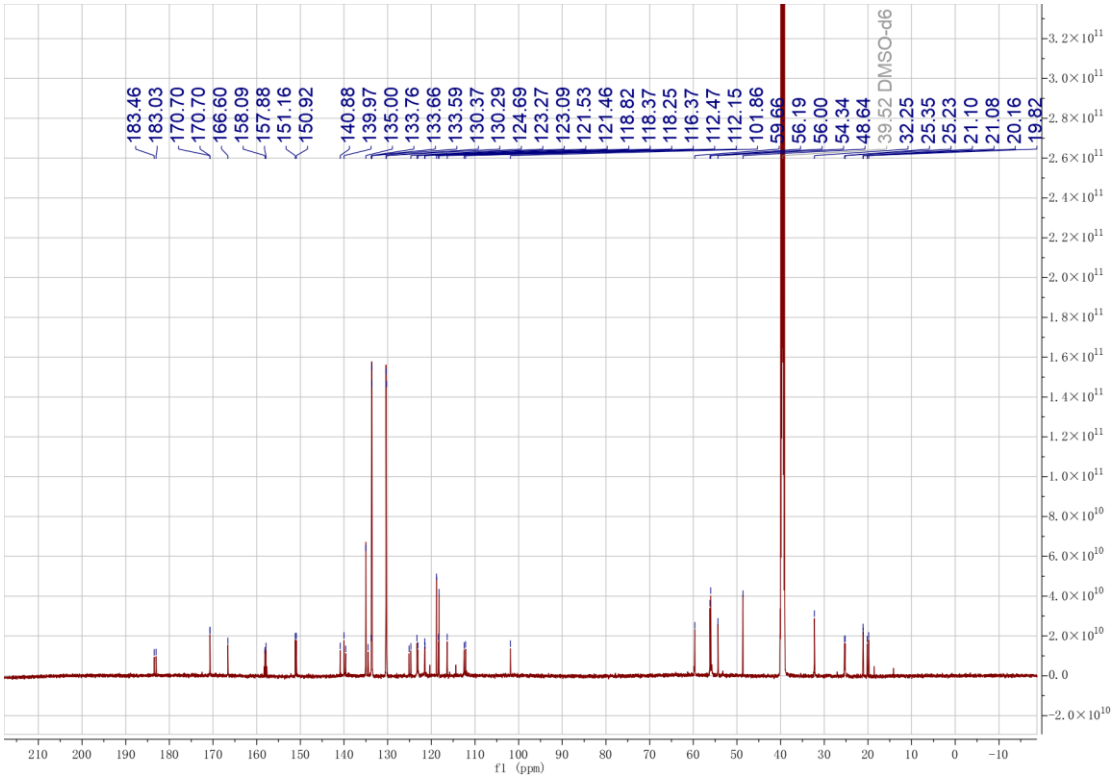

Fig. S10 ^{13}C NMR spectrum of compound 3 in $(CD_3)_2SO$. .

1.22.11. ^{31}P NMR spectrum of compound 3

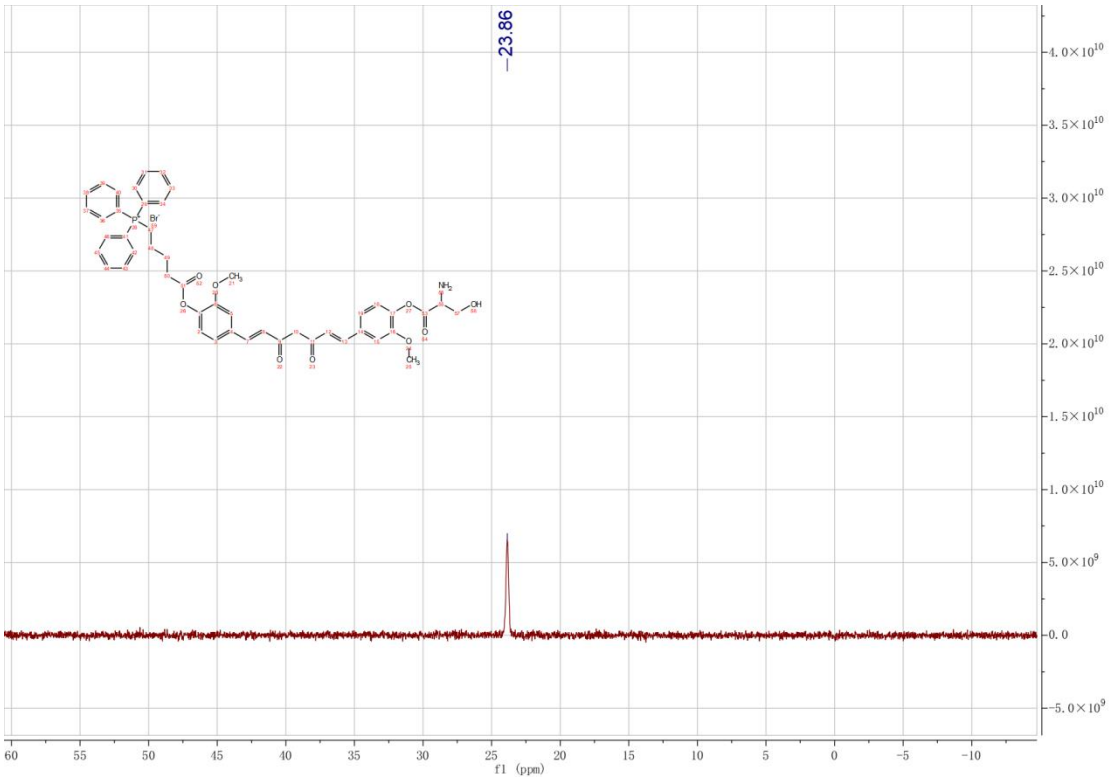

Fig. S11 ^{31}P NMR spectrum of compound 3 in $(CD_3)_2SO$.

1.22.12. ESI-HRMS of compound 3

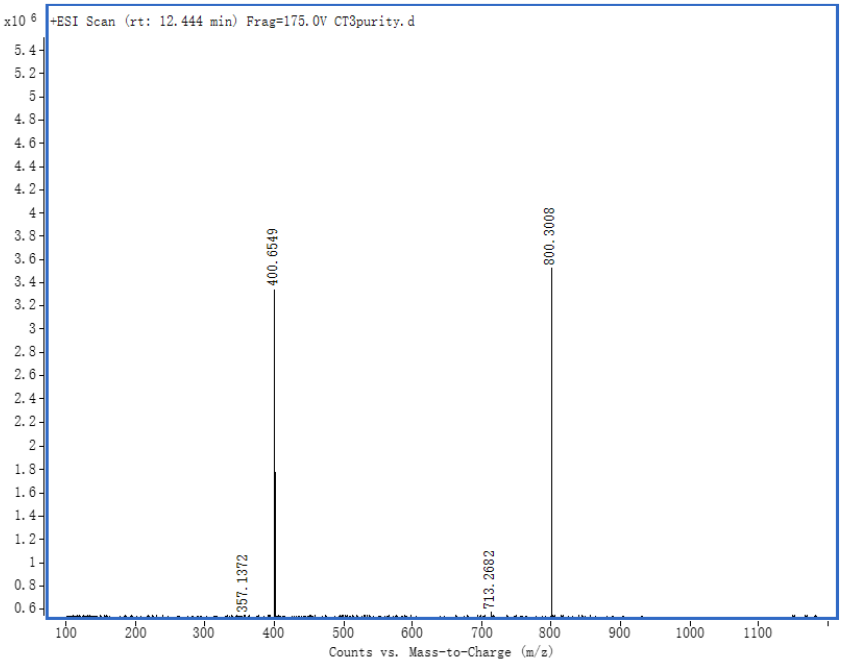

Fig. S12 ESI-HRMS of compound 3.

1.22.13. The 2D binding mode of TIM1 and L-serine

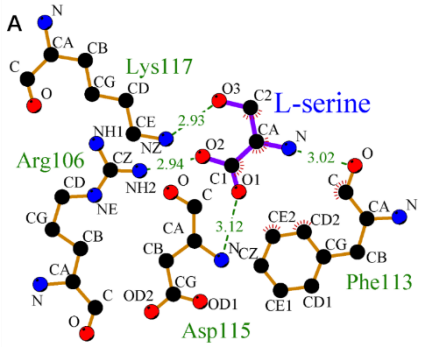

Fig. S13 The 2D binding mode of TIM1 and L-serine.

1.22.14. The 2D binding mode of TIM1 and Ser@TPP@CUR

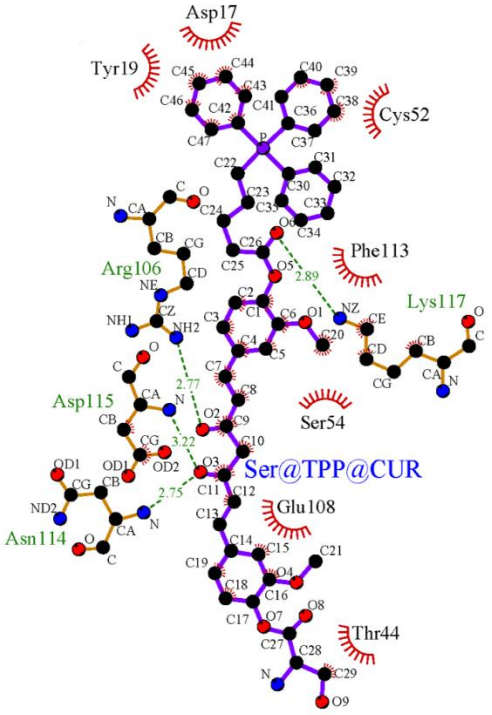

Fig. S14 The 2D binding mode of TIM1 and Ser@TPP@CUR.

1.22.15. The expression of KIM-1 receptors on HK-2 cells

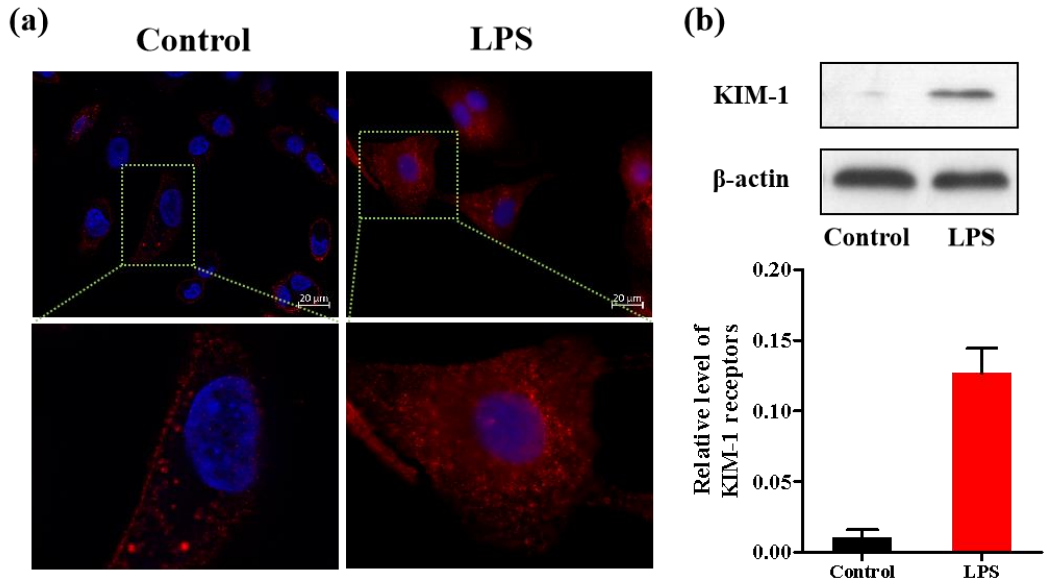

Fig. S15 The expression of KIM-1 receptors on HK-2 cells. (a) Representative fluorescent images of KIM-1 receptors on HK-2 cells with or without LPS induction. (b) Representative immunoblot of KIM-1 expression and its densitometric analysis.

1.22.16. Co-localization analysis

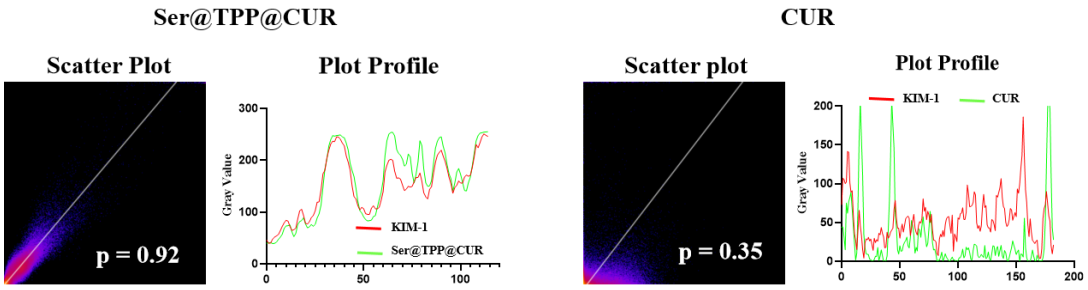

Fig. S16 Co-localization analysis of Ser@TPP@CUR (Green) with KIM-1 receptors (Red) on HK-2 cells, free CUR as control.

1.22.17. Co-localization analysis

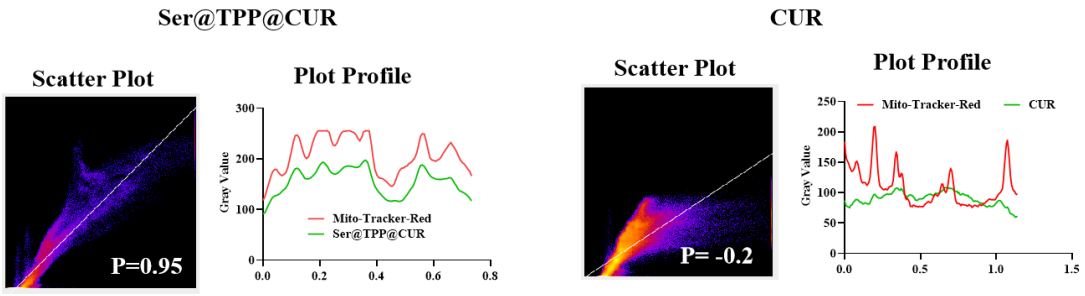

Fig. S17 Co-localization analysis of Ser@TPP@CUR with Mito-tracker Red on HK-2 cells, free CUR as control.

1.22.18. The semiquantitative fluorescence intensity

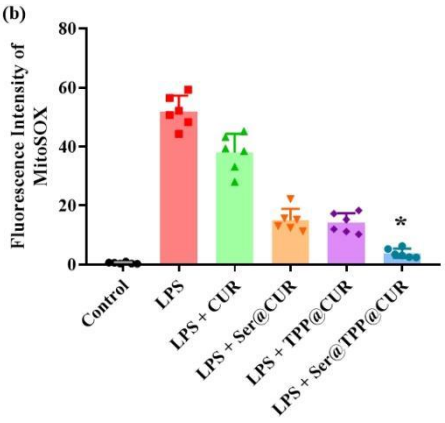

Fig. S18 The semiquantitative fluorescence intensity of MitoSOX.

1.22.19. The semiquantitative fluorescence intensity

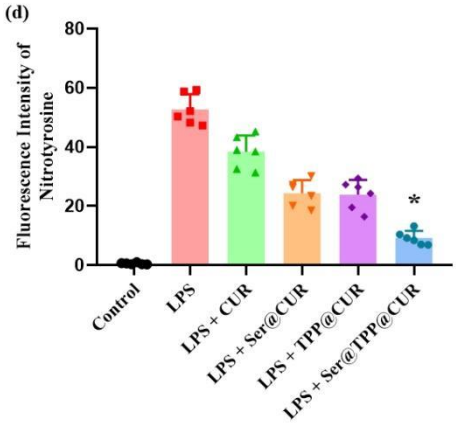

Fig. S19 The semiquantitative fluorescence intensity of nitrotyrosine expression.